Measuring proton and neutron production cross sections needed for cosmic ray studies

The initiative is funded by the Cosmochemistry program,
Office of Space Sciences
NASA

individuals have funding from both NASA and other agencies.

J. M. Sisterson. Northeast Proton Therapy Center, Massachusetts General Hospital, Boston, USA.
J. Ullmann. LANSCE, Los Alamos National Laboratory, Los Alamos, USA.
F. D. Brooks et al. Dept. of Physics, University of Cape Town, South Africa.
D. T. L. Jones et al. National Accelerator Centre, Faure, South Africa.
J. Vincent et al. TRIUMF-UBC, Vancouver, Canada.
A. J. T. Jull et al. University of Arizona, USA.
M. W. Caffee. Lawrence Livermore National Laboratory, Livermore, USA.
K. Nishiizumi. University of California, Berkeley, USA.
B. Lavielle. Centre d'Etudes Nuclearies de Bordeaux-Gradignan, France.
R. C. Reedy. Los Alamos National Laboratory, Los Alamos, USA.
J. Masarik. Comensky University, Bratslava, Slovakia.

Why measure cross sections (1) ?

• Cosmic ray particles interact with elements found in meteorites and the lunar surface to produce small quantities of radionuclides and stable isotopes.

• We can analyze these cosmogenic nuclide records to learn the history of both the object and the cosmic rays.

• Solar proton interactions are limited to the top few centimeters of an extraterrestrial object.

• Galactic cosmic rays particles (most are protons) penetrate deeply into an object and their interactions produce many neutrons. These neutrons also undergo interactions contributing to the total cosmogenic nuclide inventory.

• We need very good cross section information for the theoretical calculations used to interpret the cosmogenic nuclide records.

Why measure cross sections (2) ?

•We have good measurements for most proton production cross sections.

•We have few measurements of any of the needed neutron production cross sections.

• We are making two kinds of neutron production cross section measurements:

a) Using quasi-monoenergetic neutron beams
b) Using 'white' neutron beams.

•The information from these adjunct experiments will allow us to make better estimates of the galactic cosmic ray contribution to the total cosmogenic nuclide production.

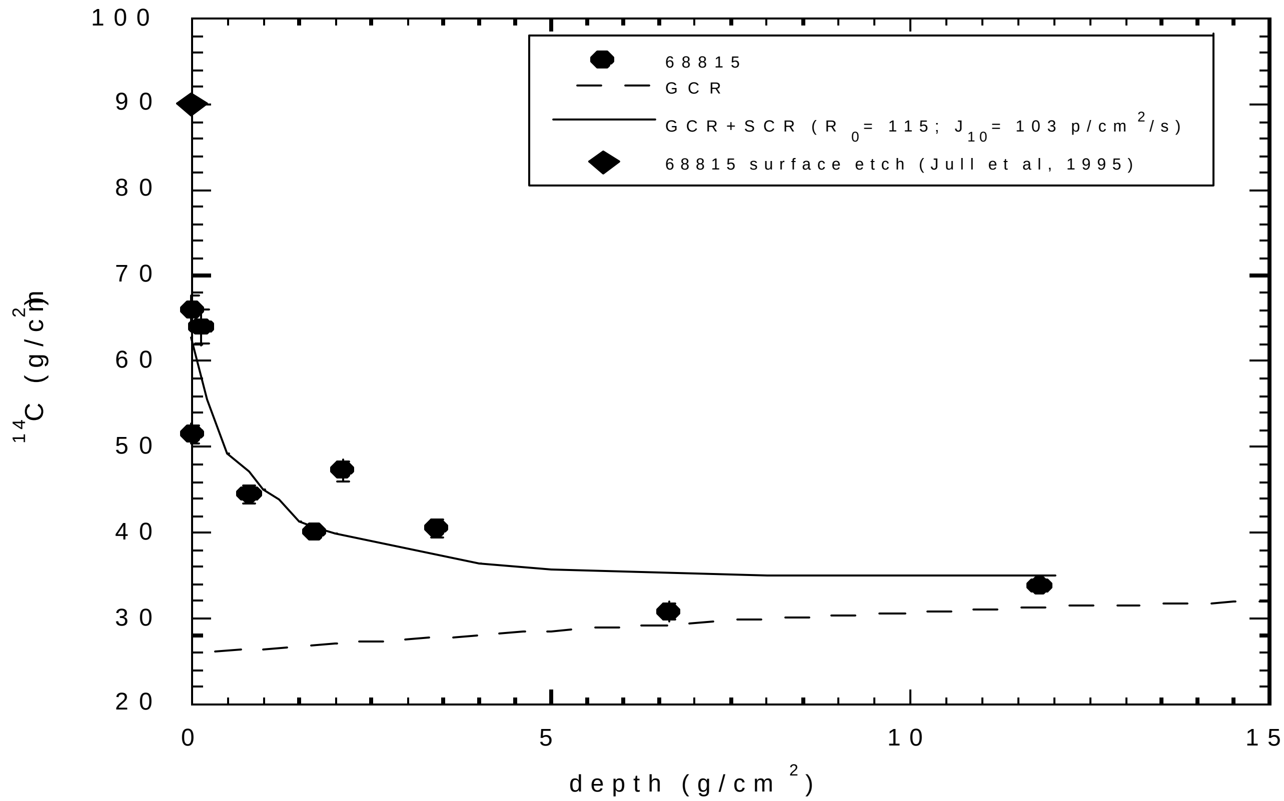

Figure 1: Taken from Jull et al.: ^{14}C (dpm/kg) as a function of depth in Apollo 16 rock 68815,292. The plot shows the experimental measurements (•) compared to the best fit of SCR of R_0 = 115 MV and J_{10} = 103 p/cm^2/s, plus GCR (solid line), as well as the calculated GCR production, plotted as the dashed line. Bulk density of the rock is 2.8 g/cm^3. Also shown is the higher surface value measured by Jull et al. in 1995, from acid etching of the rock surface. This sample shows the effects of surface implantation by solar-wind ^{14}C in the top few nanometers.

Error bars are as shown or are smaller than the symbols plotted.

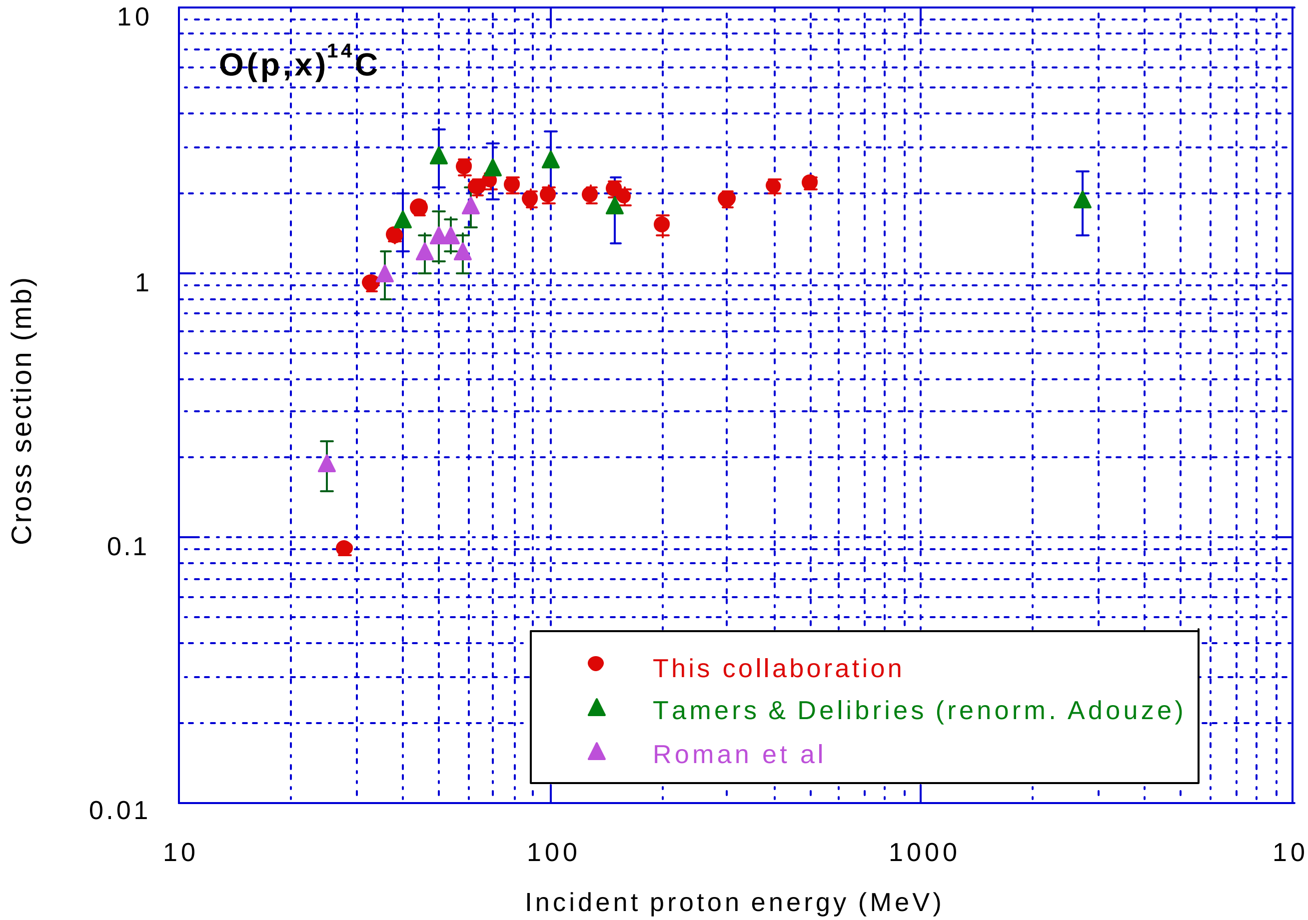

Measured at NAC 1998, as a test irradiation.
The ^{14}C AMS determination is suspect.
Incorrect flux value used in the calculation.

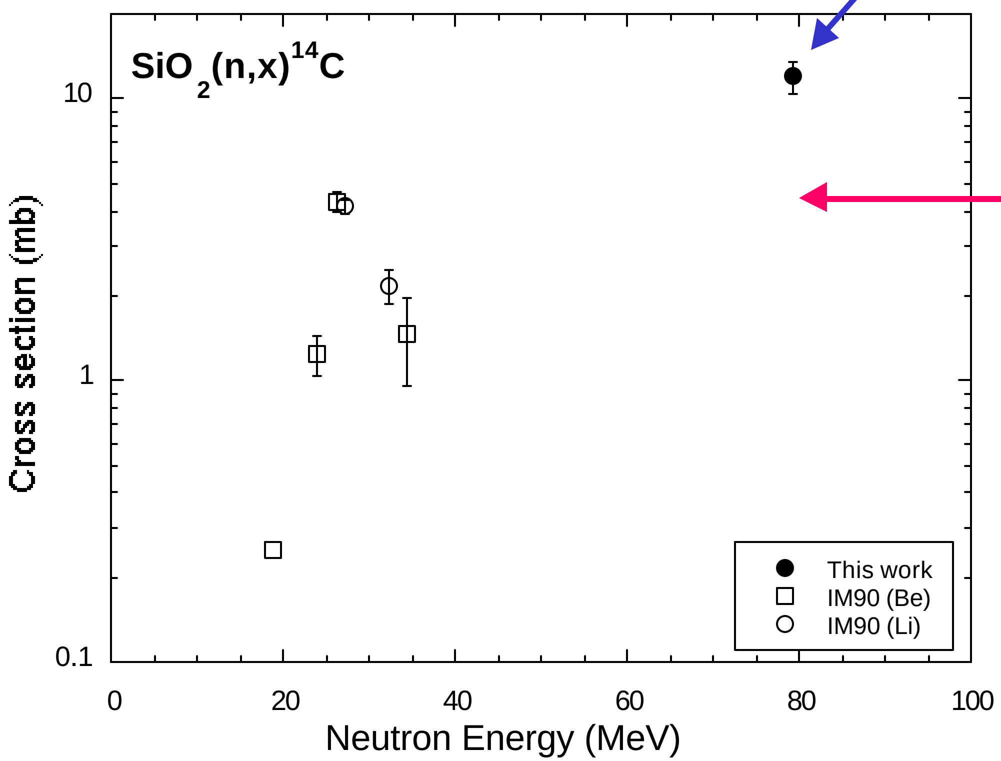

Using the corrected flux value the cross section is ~4 mb.

SiO_2 targets were irradiated at neutron energies of 76 and 114 MeV in April 1999 to measure $O(n,x)^{14}C$. Still have to do the AMS determination of ^{14}C.

Neutron (estimated, **red circles**) and proton (measured, black circles) cross sections for ^{10}**Be production from oxygen.** (Leya *et al*, 2000)

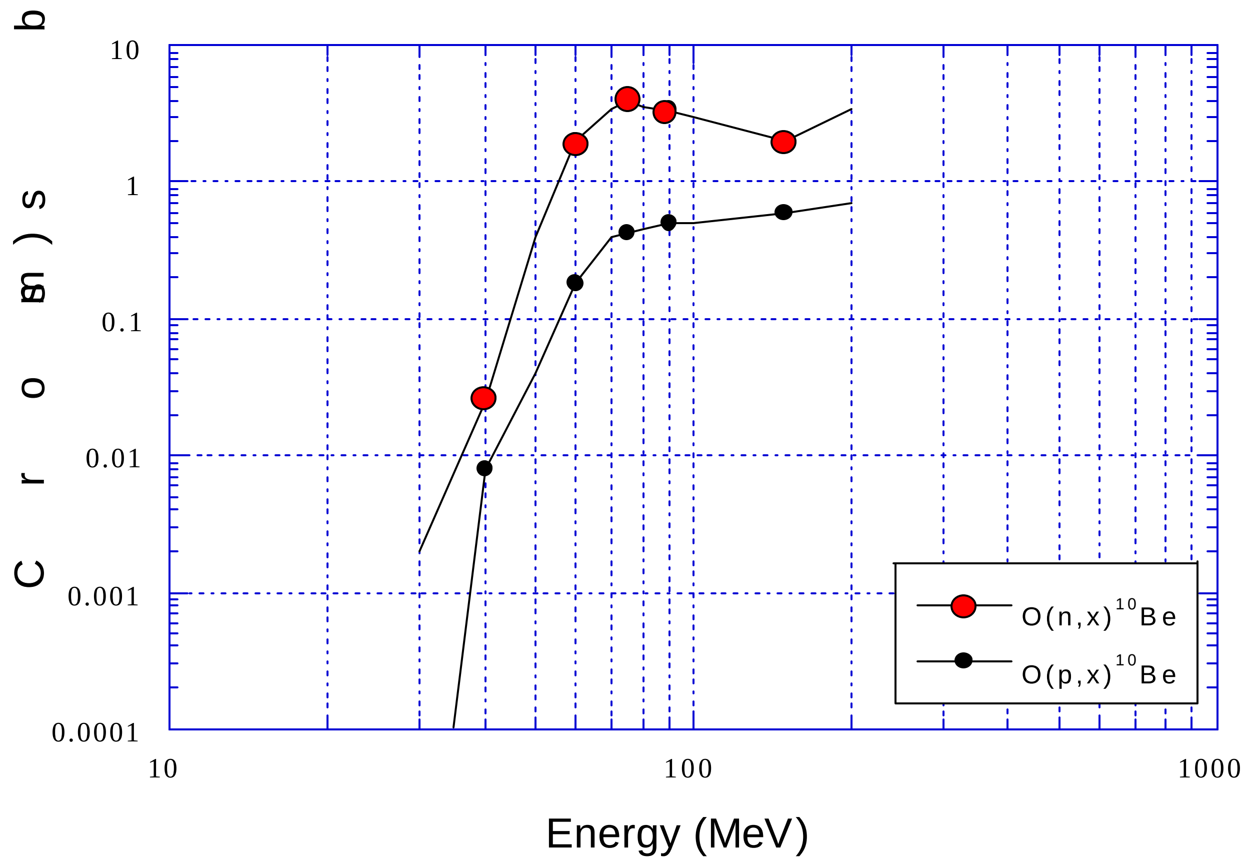

Stage 1.
Neutron calibration measurements

- Two or more neutron monitors are calibrated against a **spectrometer** which measures the absolute neutron fluence (at 0^o).
- The neutron spectra at 0^o and 16^o are compared in order to determine a “tail” correction. (see later).

These measurements are made using a low neutron intensity (beam current < 100 nA, pulse selector on) and require 5-8 hours of running.

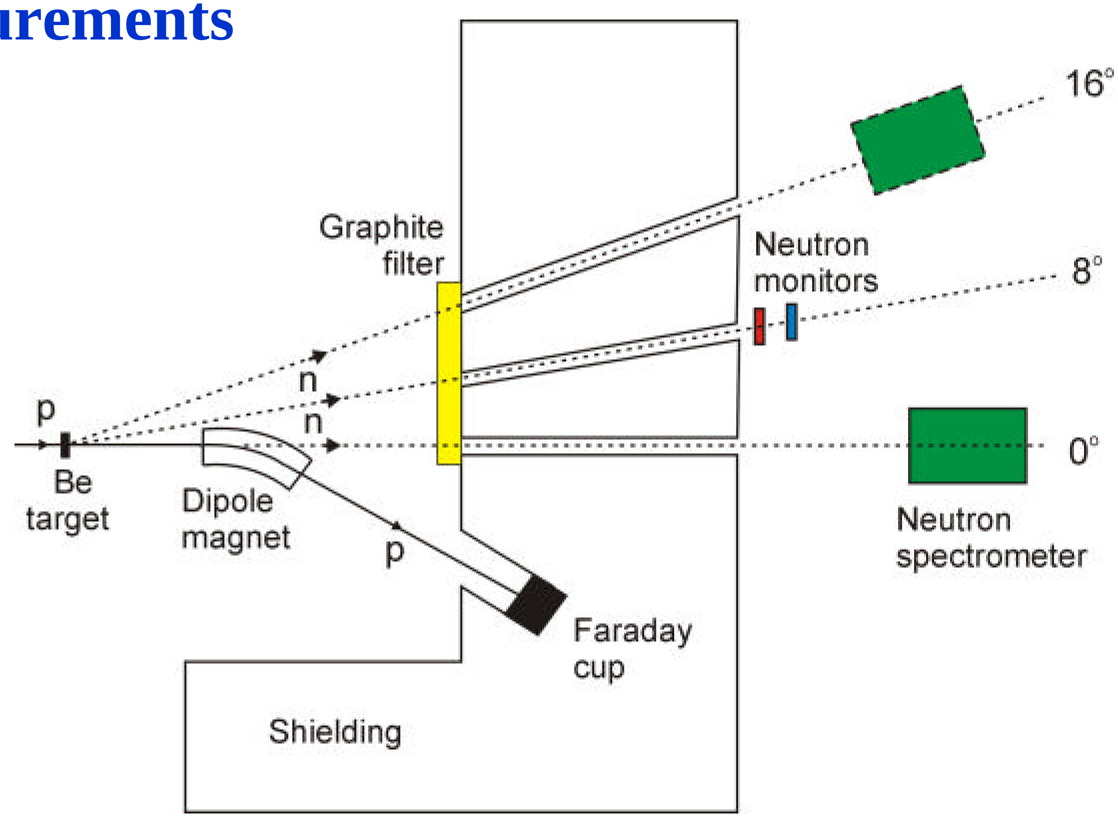

Correction for low-energy neutron "tail"

A normalization factor used in the procedure developed to correct for the low-energy tail of the neutron spectrum is determined from a comparison of neutron spectra measured on the **0°** and **16°** neutron beams.

Spectral fluence measured for 100 MeV protons on a ^{nat}Li target.

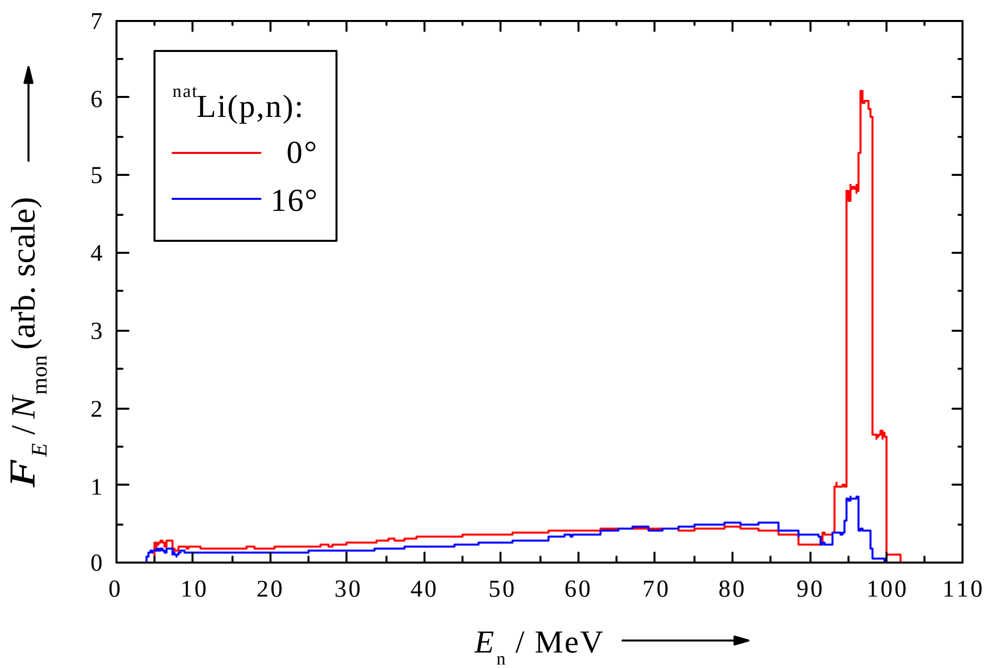

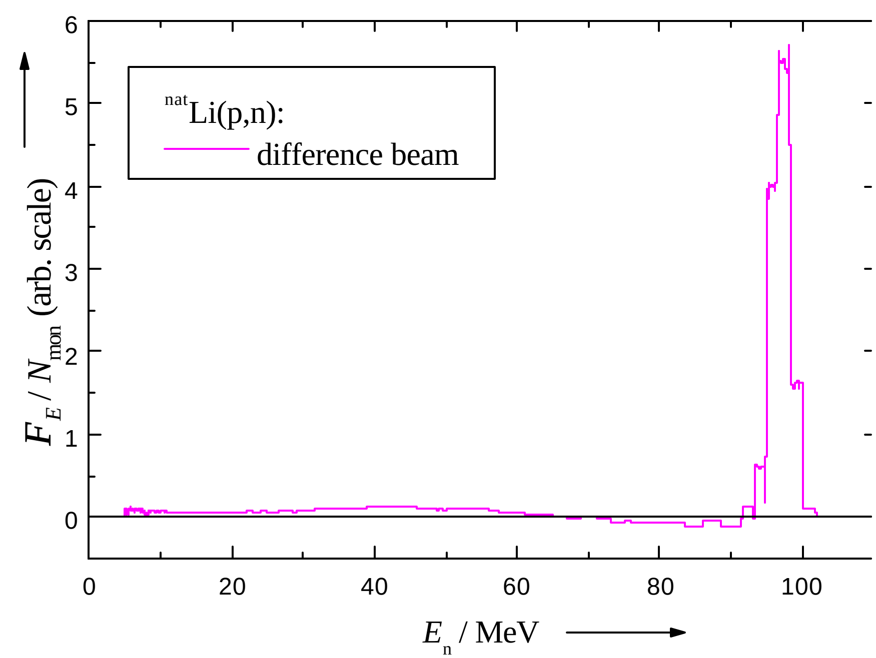

"High energy neutron reference fields for the calibration of detectors used in neutron spectrometry
R. Nolte, M.S. Allie, P.J. Binns, F.D. Brooks, A. Buffler, V. Dangendorf, J.P. Meulders, H. Schuhmacher, B. Wiegel
Presentation at the *International Workshop on Neutron Field Spectrometry in Science, Technology and Radiation Protection*, Pisa, Italy, June 2000 (Paper submitted for publication in special edition of NIM A)

Stage 2.
Target irradiation

Two identical **target stacks** are mounted in the two neutron beams (0° and 16°) and irradiated for the remainder of the weekend, using a high-intensity neutron beam (>4000 nA, pulse selector off).

The calibrated neutron monitors measure the neutron fluence.

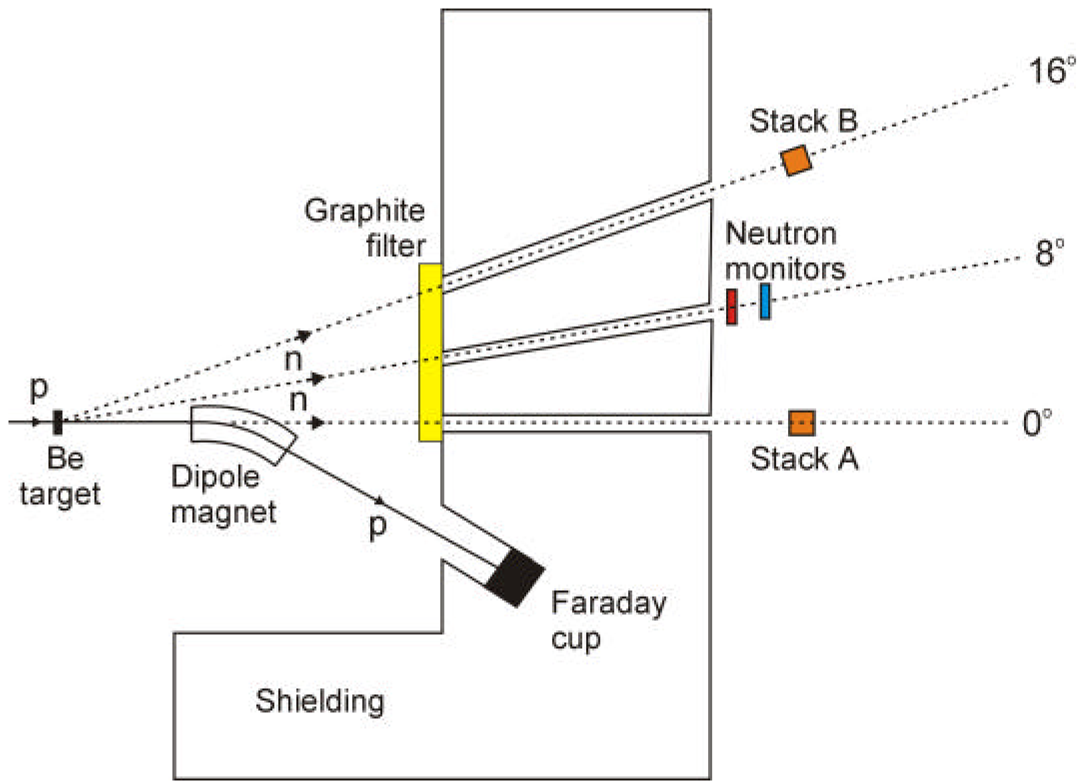

Irradiation set-up at LANSCE showing the target holder downstream of the Uranium fission chamber used to monitor the beam. The 1998 target holder is shown. Monitor foils are included in the target stack to study possible monitor cross sections.

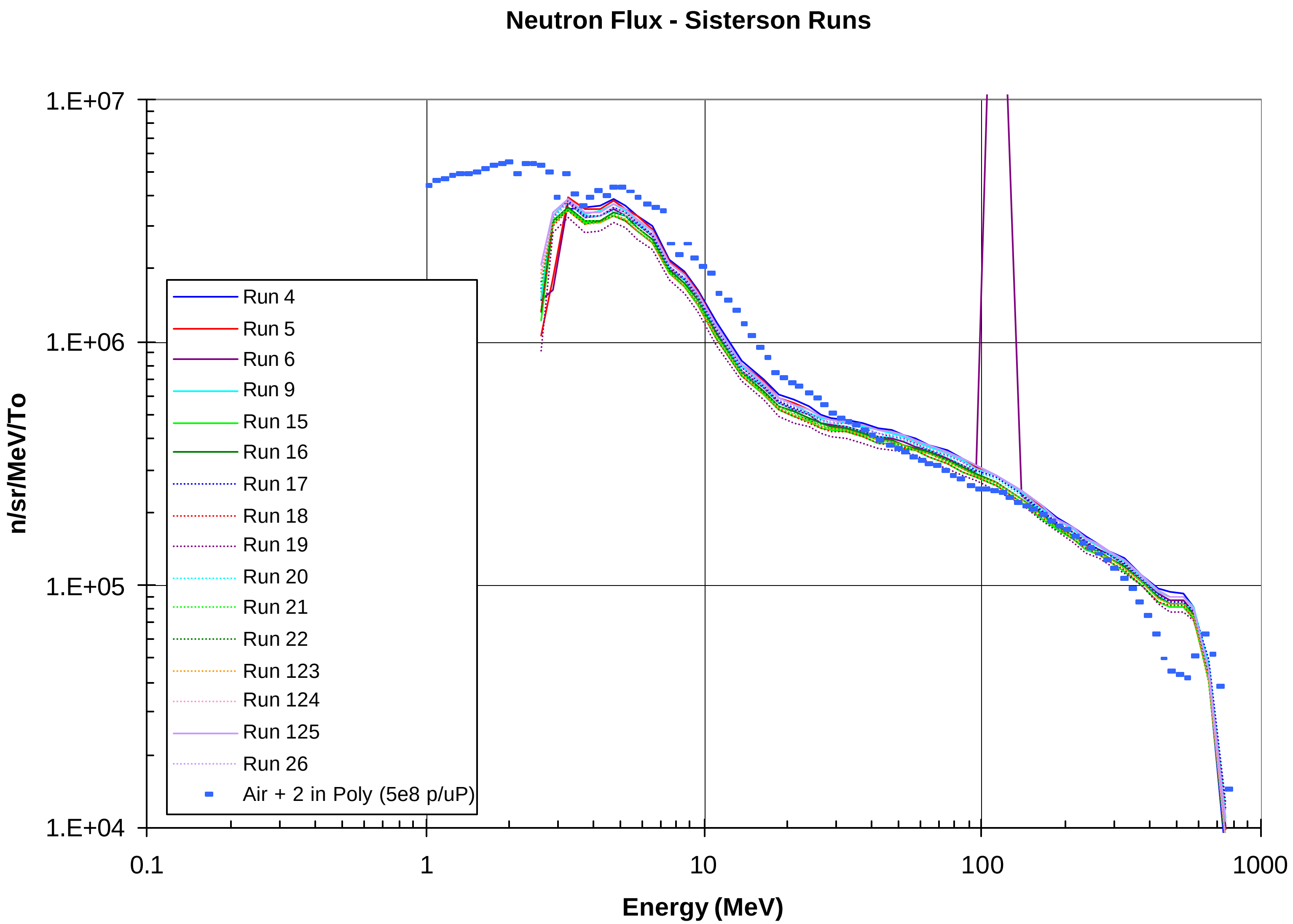

Neutron energy spectra for the Fe and Ni irradiations at LANSCE in November 1999, including an obvious computer glich.

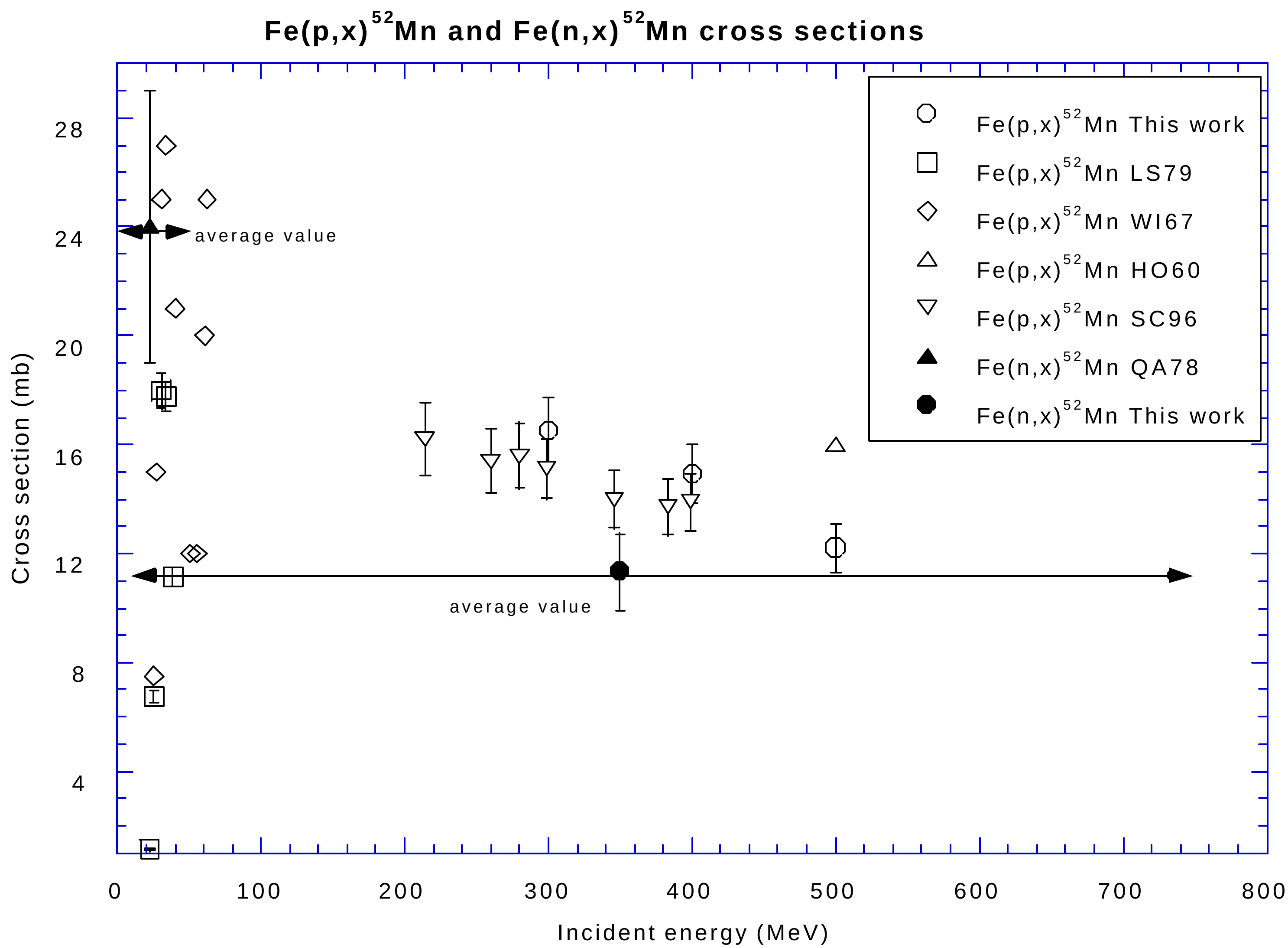

Fe(p,x)^{52}Mn and Fe(n,x)^{52}Mn cross sections
Cross section (mb)
Incident energy (MeV)
0
100
200
300
400
500
600
700
800
4
8
12
16
20
24
28
average value
average value
Fe(p,x)^{52}Mn This work
Fe(p,x)^{52}Mn LS79
Fe(p,x)^{52}Mn WI67
Fe(p,x)^{52}Mn HO60
Fe(p,x)^{52}Mn SC96
Fe(n,x)^{52}Mn QA78
Fe(n,x)^{52}Mn This work

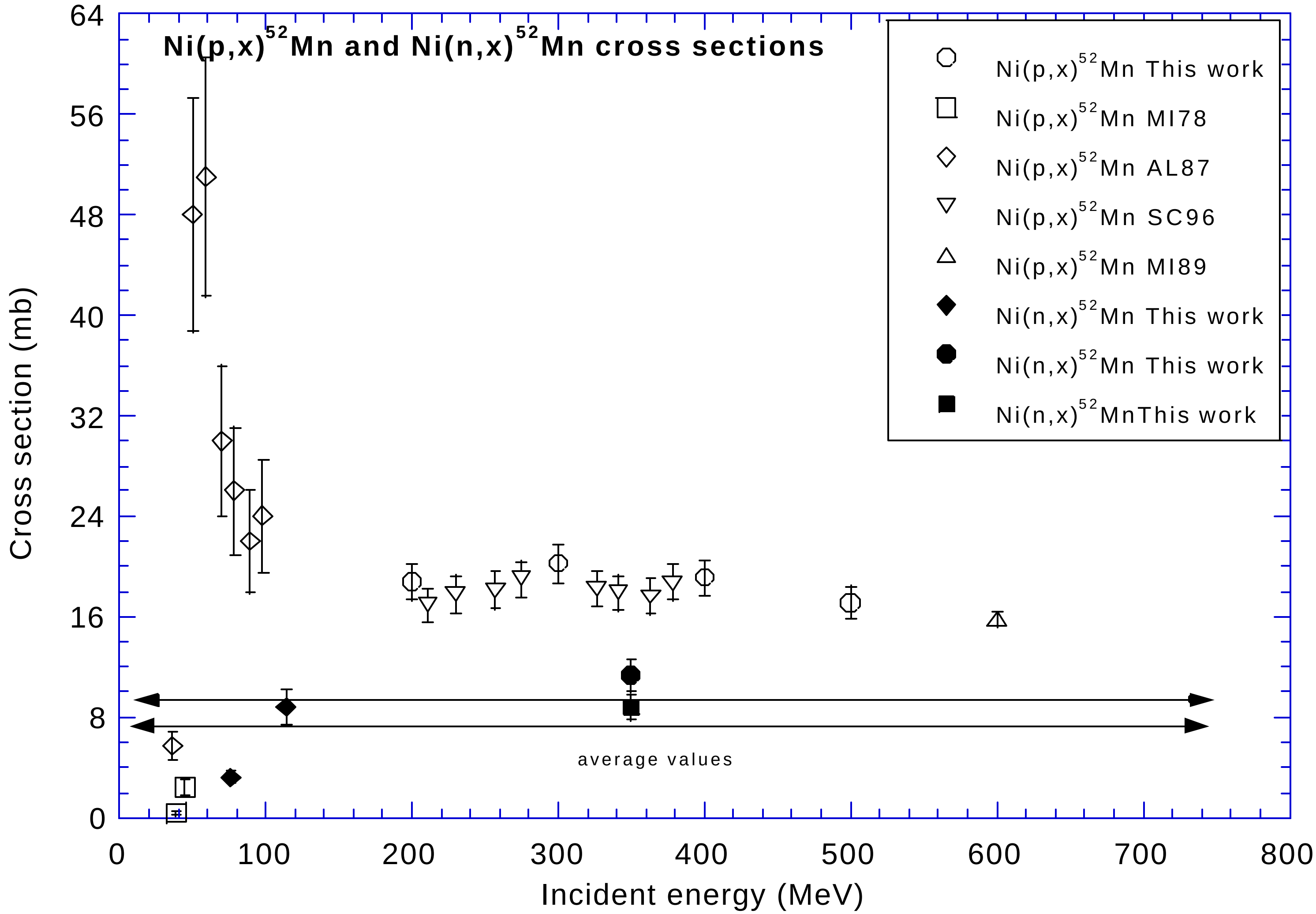

Ni(p,x)52Mn and Ni(n,x)52Mn cross sections
Ni(p,x)52Mn This work
Ni(p,x)52Mn MI78
Ni(p,x)52Mn AL87
Ni(p,x)52Mn SC96
Ni(p,x)52Mn MI89
Ni(n,x)52Mn This work
Ni(n,x)52Mn This work
Ni(n,x)52MnThis work
average values
Cross section (mb)
Incident energy (MeV)
0
8
16
24
32
40
48
56
64
0
100
200
300
400
500
600
700
800

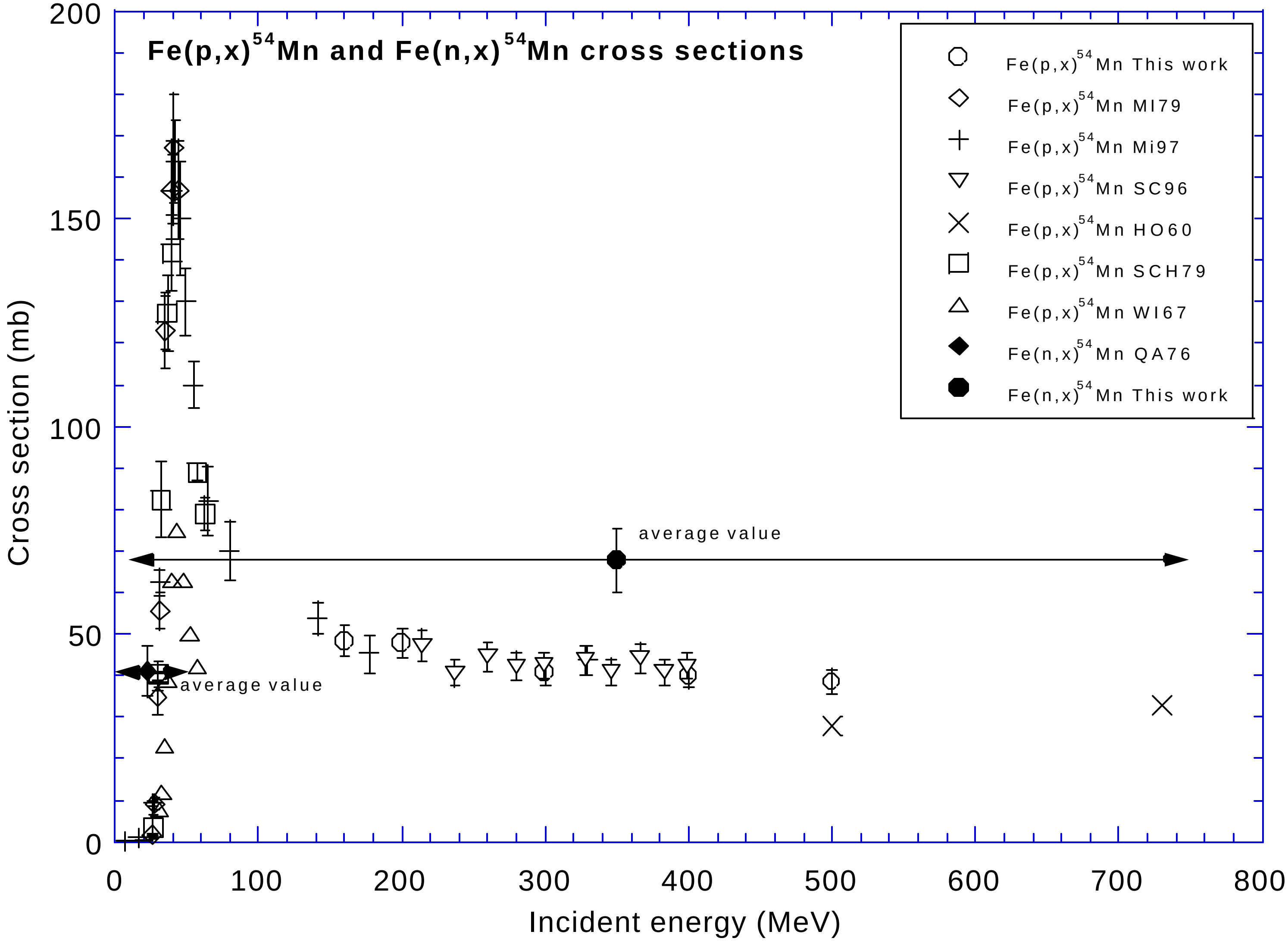

Fe(p,x)54Mn and Fe(n,x)54Mn cross sections
Fe(p,x)54Mn This work
Fe(p,x)54Mn MI79
Fe(p,x)54Mn Mi97
Fe(p,x)54Mn SC96
Fe(p,x)54Mn HO60
Fe(p,x)54Mn SCH79
Fe(p,x)54Mn WI67
Fe(n,x)54Mn QA76
Fe(n,x)54Mn This work
average value
average value
Cross section (mb)
Incident energy (MeV)
0
50
100
150
200
0
100
200
300
400
500
600
700
800

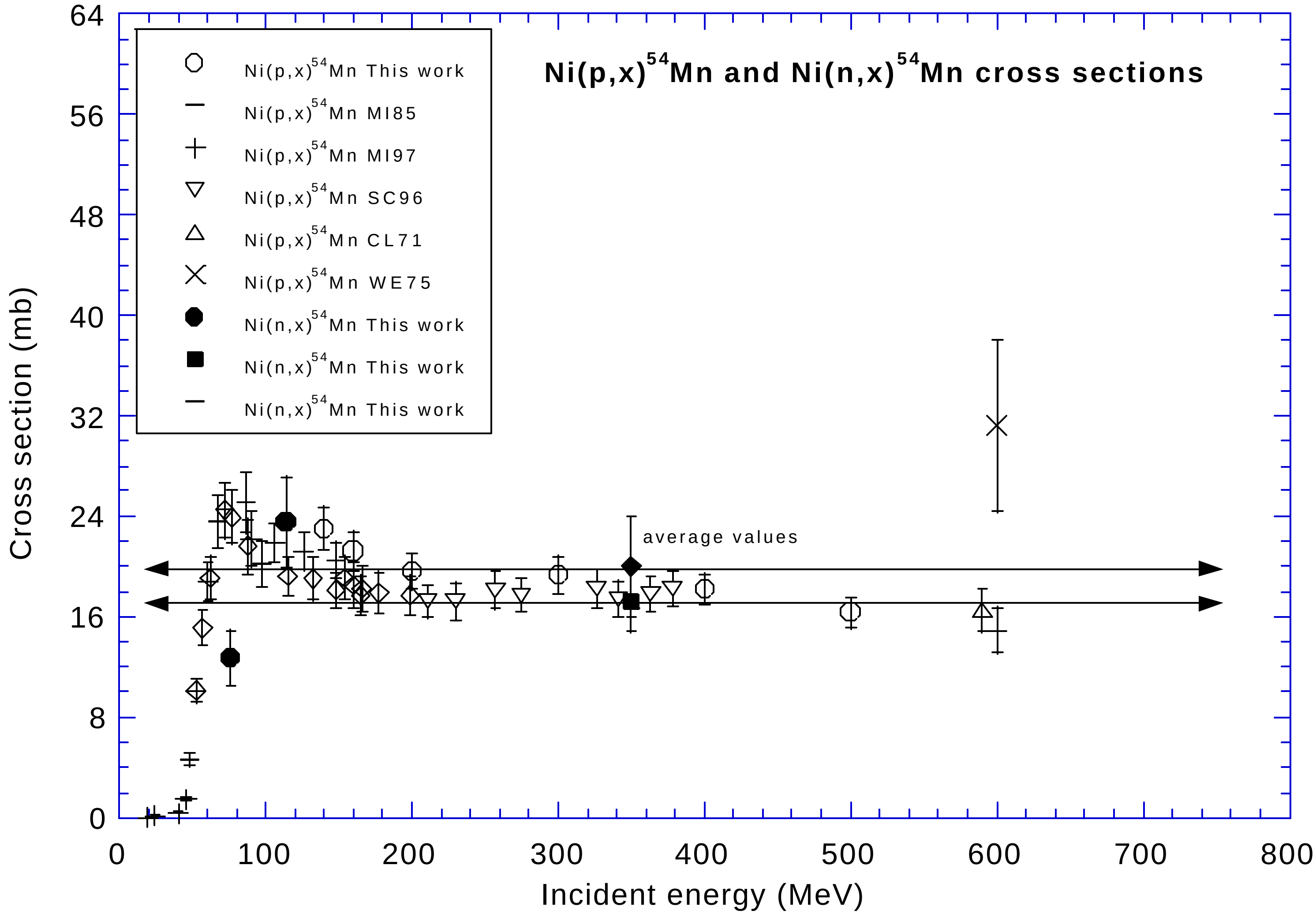

Ni(p,x)54Mn and Ni(n,x)54Mn cross sections
Ni(p,x)54Mn This work
Ni(p,x)54Mn MI85
Ni(p,x)54Mn MI97
Ni(p,x)54Mn SC96
Ni(p,x)54Mn CL71
Ni(p,x)54Mn WE75
Ni(n,x)54Mn This work
Ni(n,x)54Mn This work
Ni(n,x)54Mn This work
average values
Cross section (mb)
Incident energy (MeV)
0
8
16
24
32
40
48
56
64
0
100
200
300
400
500
600
700
800

Extinct radioactivities in meteorites (1)

•Fluctuating x-winds might revive an earlier explanation for the extinct radioactivities found in meteorities. The bombardment of rocks by cosmic rays from the young sun.

•Conventionally, this idea foundered because a p + alpha flux sufficient to produce ^{41}Ca and ^{53}Mn at the level found in meteorites failed by about 2 orders of magnitude to produce enough ^{26}Al.

•However, impulsive flares arising from reconnection events in the reconnection ring, where CAI precursors lie before they are launched by an inwardly encroaching x-wind, accelerate numerous ^{3}He nuclei to mega-electron volts per nucleon and higher energies.

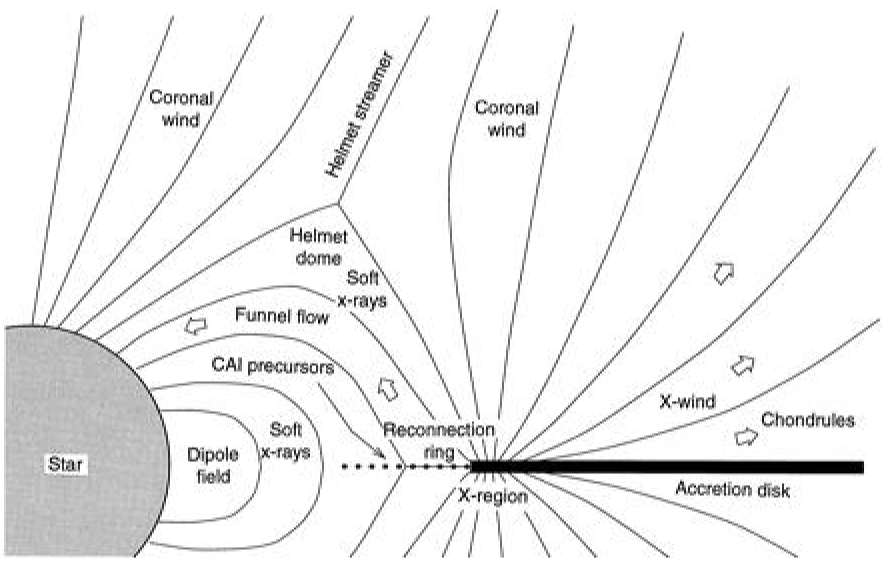

•CAIs are Ca-Al-rich inclusions of primitive cbondrite meteorites and are the oldest solar system materials, which crystallized in the solar nebula.

•Recently, evidence for ^{10}Be in-situ decay in CAIs was found. ^{10}Be is only produced by spallation reactions, so its existence in early solar system materials indicates that there is intense irradiation processes in the solar nebula.